Paper Published

1. **Souvik Nandi**, Abinash Ojha, Ashirbad Nanda,Rudra Narayan Sahoo, Rakesh Swain, Krushna Prasad Pattnaik and Subrata Mallick. Vildagliptin plasticized hydrogel film in the control of ocular inflammation after topical application: study of hydration and erosion behaviour. Zeitschrift für Physikalische Chemie. 2021; Just Accepted: https://doi.org/10.1515/zpch-2021-3081 [Impact Factor 2.4]

2. **Souvik Nandi**, Satyaki A Mishra, Rudra N Sahoo, Rakesh Swain, Subrata Mallick. Influence of TiO2 on Mucosal Permeation of Aceclofenac: Analysis of Crystal Strain and Dislocation Density. Acta Chimica Slovenica. 2020;67(4):1227-32. [Impact Factor: 1.735] [http://dx.doi.org/10.17344/acsi.2020.6129]

3. **Souvik Nandi**, Mishra SA, Sahoo RN, Swain R, Mallick S. Quantitative Estimation of Tabletability of Aceclofenac after Incorporation of Titanium Dioxide using Area under the Curve. Indian Journal of Pharmaceutical Education and Research. 2020 Jan 1;54(1):68-72. [Impact Factor: 0.686] [http://dx.doi.org/10.5530/ijper.54.1.8]

4. Satapathy SR, Sahoo RN, **Nandi S**, Satapathy B, Panigrahi L, Mallick S. 3D printing in managing supply disruptions related to COVID-19 pandemic: Food and Drug Administration's current thinking on regulation. Minerva Biotecnologica. 2021:43-.[Impact Factor: 3.028] [http://dx.doi.org/10.23736/S2724-542X.20.02730-5]

5. Pramanik A, Sahoo RN, **Nandi S**, Nanda A, Mallick S. Characterization of Hydration Behaviour and Modeling of Film Formulation. Acta Chimica Slovenica. 2021 Mar 20;68(1):159-69. [Impact Factor: 1.735] [http://dx.doi.org/10.17344/acsi.2020.6298]

6. Pattanaik S, **Nandi S**, Sahoo RN, Nanda A, Swain R, Das S, Mallick S. Budesonide-cyclodextrin in hydrogel system: impact of quaternary surfactant on in vitro-in vivo assessment of mucosal drug delivery. Rev Chim. 2020;71:332-45. [Impact Factor: 1.755, 2020] [http://dx.doi.org/10.37358/RC.20.6.8200]

7. Dash R, Sahoo RN, **Nandi S**, Swain R, Mallick S. Sustained Release Bioadhesive Suppository Formulation for Systemic Delivery of Ornidazole: In-silico Docking Study. Indian Journal of Pharmaceutical Education and Research. 2019 Oct 1;53(4):S580-6. [Impact Factor: 0.686] [http://dx.doi.org/10.5530/ijper.53.4s.153]

8. Sahoo RN, Nanda A, Pramanik A, **Nandi S**, Swain R, Pradhan SK, Mallick S. Interactions between Ibuprofen and Silicified-MCC: characterization, drug release and modeling approaches. Acta Chimica Slovenica. 2019 Dec 18;66(4):923-33. [Impact Factor: 1.735] [http://dx.doi.org/10.17344/acsi.2019.5139]

9. Swain R, **Nandi S**, Sahoo RN, Swain S, Mohapatra S, Mallick S. Bentonite clay incorporated topical film formulation for delivery of trimetazidine: Control of ocular pressure and in vitro-in vivo correlation. Journal of Drug Delivery Science and Technology, 2021 (Just Accepted) [Impact Factor: 3.981]

Souvik Nandi, Abinash Ojha, Ashirbad Nanda,
Rudra Narayan Sahoo, Rakesh Swain, Krushna Prasad Pattnaik
and Subrata Mallick*

Vildagliptin plasticized hydrogel film in the control of ocular inflammation after topical application: study of hydration and erosion behaviour

https://doi.org/10.1515/zpch-2021-3081
Received June 25, 2021; accepted July 25, 2021; published online August 6, 2021

Abstract: Vildagliptin (VID) is a dipeptidyl peptidase-4 (DPP-4) inhibitor used in controlling blood glucose level in type 2 diabetes. Vildagliptin improves beta cells function and is also suggested to effectively control the inflammation. The possible ocular anti-inflammatory property of vildagliptin has been explored using topically applied plasticized ocular film formulation. Film formulation was prepared by solvent cast and evaporation method using triethanolamine (TEA), dimethyl sulphoxide (DMSO), and polyethylene glycol 400 (PEG 400) as the plasticizer in HPMC hydrogel matrix base. Anti-inflammatory study was carried out in the carrageenan induced ocular rabbit model. Analytical methods confirmed that the drug was present almost in completely amorphized form in the film formulation. Level of hydration, swelling and erosion rate of the film played the controlling factor in the process of drug release, ocular residence and permeation. Maximum swelling rate of 363 h^{-1} has been shown by VHT compared to other formulation of VHD and VHP (174 and 242 h^{-1} respectively). Film containing DMSO exhibited highest *in vitro* release as well as *ex vivo* ocular permeation. Film formulation has shown a fast recovery of ocular inflammation in contrast to the untreated eye after inducing inflammation. Plasticized vildagliptin hydrogel film formulation could be utilized in the management and control of ocular inflammation particularly

***Corresponding author: Subrata Mallick**, School of Pharmaceutical Sciences, Siksha 'O' Anusandhan (Deemed to be University), Bhubaneswar 751003, India,
E-mail: profsmallick@gmail.com
Souvik Nandi, Abinash Ojha, Ashirbad Nanda, Rakesh Swain and Krushna Prasad Pattnaik, School of Pharmaceutical Sciences, Siksha 'O' Anusandhan (Deemed to be University), Bhubaneswar 751003, India
Rudra Narayan Sahoo, School of Pharmaceutical Sciences, Siksha 'O' Anusandhan (Deemed to be University), Bhubaneswar 751003, India; and School of Pharmacy and Life Sciences, Centurion University of Technology and Management, Odisha, India

with diabetic retinopathy after proper clinical studies in higher animal and human individuals.

Keywords: diabetes; DPP-4 inhibitor; film plasticizer; hydrogel; ocular anti-inflammation; vildagliptin.

1 Introduction

Vildagliptin (VID), a potent orally active dipeptidyl peptidase-4 (DPP-4) inhibitor is used for the treatment of type 2 diabetes mellitus [1–3]. Increased risk of cardiovascular disease, hepatitis-C infection and pancreatitis is reported in the people with diabetes [4]. Despite of an oral bioavailability of 85% it has shorter elimination half-life of 1.5 h. Being DPP-4 inhibitor vildagliptin is known to effectively control the inflammation besides improving beta cells function [5, 6]. The possible anti-inflammatory property of vildagliptin may add the additional value in the patients particularly with diabetic retinopathy [7].

Diabetes Mellitus (Type-2) is one of the most common health problems worldwide which is expected to reach 592 million patients by 2035 [8]. Cho et al. 2018 reported that more than 250 million people already affected by Type 2 Diabetes Mellitus [9]. The main cause of Type 2 Diabetes is a result of insulin resistance and impairment of insulin secretion from β cells [10]. Gliptin class of dipeptidyl peptidase-4 (DPP-4) inhibitors can effectively control the inflammation which occurs simultaneously with type-2 diabetes mellitus inflammation in the pancreatic beta cell [11–14].

Topical medication exerts low risk of systemic adverse effects and drug interactions. Topical delivery systems promote localized action and avoid systemic toxicity bypassing the first-pass metabolism [15]. Ocular hydrogel films are very much suitable for controlled ophthalmic drug delivery [16–18]. Polymeric hydrogel films have the capability of swelling after hydration in the tear fluid and form bond with the mucin protein chains, and increase the contact time in the site of action. Hydrogel formulations also overcome the nasolacrimal drainage problem associated with liquid ophthalmic drops exhibiting significantly low bioavailability [19]. Eye ointment is viscous and can increase the residence time but patient acceptability is less due to blurred vision, sticky eyes and uncomfortable feelings [20]. Hydroxypropyl methylcellulose (HPMC), a hydrogel forming polymer is very much suitable for ocular drug delivery formulation [21]. It is non-irritant to the eye and maintains inertness when used with a wide range of drugs in the ocular delivery systems. According to recent reports HPMC is also being used in the case of ophthalmic delivery.

Triethanolamine (TEA), Dimethyl sulphoxide (DMSO), and Polyethylene glycol 400 (PEG 400) have been used as plasticizer in the ocular film formulation [22–24]. The effect of plasticizer on the *in vitro* drug release and *ex vivo* corneal permeation has been studied. The possible ocular antiinflammatory study was examined on carrageenan induced rabbit eye model.

2 Materials and methods

2.1 Material

Vildagliptin (MW: 303.399 g/mol) was a gift sample provided by Glenmark Pharmaceutical Ltd (Mumbai). Hydroxypropyl methylcellulose HPMC K15M: Qualikems (Vadodara), TEA: Burgoyne Urbidges & Co. (Mumbai), DMSO and PEG 400: MERCK. Carrageenan was purchased from Himedia Laboratories Pvt. Ltd.

2.2 Vildagliptin film formulation

HPMC was soaked with distilled water and refrigerated for 24 h for complete hydration and swelling. Vildagliptin and plasticizer (triethanolamine, dimethyl sulphoxide or PEG 400) were added to the swelled mass and stirring was continued for 12 h using magnetic stirrer [25, 26]. The gel-like mass was then poured in a petridish and placed in an incubator at 45 °C for 24 h for drying upto constant weight [27].

2.3 Thickness and folding endurance

The thickness of the prepared film formulations was measured by digital micrometer (Mitutoyo, Japan). An average reading was taken after measuring the film thickness at various places. Folding endurance of the film was then tested till the film breaks apart and the result was recorded [28].

2.4 Swelling and erosion study

The hydration and swelling of 1 × 1 cm pre-weighed film piece was carried out on a glass slide. About 40 ml of simulated tear fluid (pH 6.8) was poured on the glass slide and weighed at regular time interval after wiping out the excess phosphate buffer solution [29]. The hydration percentage was calculated by using the following formula.

$$\text{Dynamic hydration (\%)} = \frac{(\text{weight after hydration} - \text{initial dry weight before hydration})}{\text{Hydrated weight}} \times 100$$

The swelling rate (K_s) was calculated by slope of the linear profile of % swelling index versus time plot.

Erosion study was done by placing the hydrated films in an oven overnight at 60 °C. The film was then placed over activated silica in the desiccator gel for 24 h in order to remove moisture, if any. The difference between the initial weight and the dried weight was taken to estimate the erosion percentage using following formula:

$$\%\ \text{Erosion} = \frac{(\text{dry weight before hydration} - \text{dry weight after after hydration})}{\text{dry weight before hydration}} \times 100$$

2.5 Moisture content and uptake

The initial weight of a piece of the prepared film was taken and kept in a desiccator over activated silica gel. The film was then weighed after 24 h and the weight difference was used to evaluate the moisture content value.

$$(\%)\ \text{Moisture Content} = \frac{(\text{Final weight} - \text{initial weight})}{\text{Final weight}} \times 100$$

A pre-weighed film was placed in a closed desiccator maintained at the relative humidity of 75% and the final weight was taken after achieving equilibrium (till constant weight). A head space of 75% relative humidity was maintained inside the closed desiccator containing supersaturated NaCl slurry [30]. Moisture uptake of the film was estimated using the following formula:

$$(\%)\ \text{Moisture uptake} = \frac{(\text{Final weight} - \text{initial weight})}{\text{intial weight}} \times 100$$

2.6 Drug content estimation

Accurately weighed randomly cut pieces of the film formulation were dissolved in phosphate buffer solution (pH 6.8) and sonicated for 1 h to obtain a clear solution. For estimating drug content the solution was made ready by passing through a syringe driven filter (0.22 µm, Whatman Uniflo). Absorbance was measured at 197 nm in UV spectrophotometer (JASCO V-630 spectrophotometer).

2.7 Fourier transform infrared spectroscopy

FTIR spectra of the pure drug as well as of the prepared films were carried out. The formulated films were cut into very fine pieces and subjected to KBr pellet method. The scan was done in the region of 4000–400 cm^{-1} in JASCO FTIR 4100 (type A) and an average of 80 scans was taken.

2.8 X-ray diffraction

X-ray diffraction has been studied for the crystal structure analysis of the pure drug and the film formulation. Any changes in the crystalline intensities in the films have been confirmed in this study. The diffraction pattern was recorded using the powder X-ray diffractometer (Rigaku, Ultima IV) equipped with a Cu X-ray source radiation wavelength of 1.5406 Å. Diffraction was measured at a scan speed of 1° per min in between 5 and 70° 2θ applying 40 kV as voltage and 15 mA as current.

2.9 Differential scanning calorimetry

Differential Scanning Calorimetry measurements were performed for the powder drug and the films. Sample weight was taken in the range of 2–3 mg for the analysis. The sample was placed in a sealed aluminum sample holder having a single perforation in the lid to eliminate the vapor which was most likely to be generated during the process. The whole operation was done under a nitrogen atmosphere to maintain inertness during the thermal analysis (METTLER TOLEDO DSC 1, STAR^e SYSTEM).

2.10 *In vitro* drug release study

The *in vitro* release study was carried out in USP type 2 paddle type dissolution apparatus (Electrolab, dissolution tester USP, TDT06L, India) [31]. Accurately weighed piece of film was fixed on a glass slide by using cyanoacrylate adhesive which then fully merged into the simulated tear fluid (phosphate buffer: pH 7.4). The bath temperature was set at 34.0 ± 0.5 °C with a paddle rotation speed of 50 rpm [30, 32, 33]. Aliquots were drawn at predetermined time intervals, passed through a syringe driven filter of 0.45 µm. The filtered liquid was then analyzed at 197 nm.

2.11 *Ex vivo* permeation study

Freshly excised goat eyes were collected from the local slaughter house in phosphate buffer (pH 6.8) for the study [34]. The undamaged corneas were separated and rinsed thoroughly in phosphate buffer (pH 6.8). The ocular membranes then attached to the modified franz diffusion cell. The *ex vivo* ocular permeation study then carried out in 200 ml of phosphate buffer medium (pH 6.8) at 34 ± 0.2 °C. Aliquots were drawn in particular time intervals and replenished with fresh medium which then subjected to UV–V is spectra analysis. The procedure was continued for 6 h [31, 35].

The permeability co-efficient (P_{ss}) was calculated by:

$$P_{ss} = \frac{J_s}{C}$$

where, J_s the flux at the steady-state, C the concentration of the drug in the film.

2.12 Anti-inflammatory activity study

The animal experimentation were approved by the institutional animal ethical committee (IAEC) [IAEC/SPS/SOA/03/2019; dated: 29th June, 2019]. The guidelines of the Committee for the Purpose of Control and Supervision of Experiments on Animals (CPCSEA), India were followed [Institution registration number: 1171/PO/RE/S/08/CPCSEA].

New-zealand white rabbit (*Oryctolagus cuniculus*) of average weight of 1.6–2.0 kg was kept in the laboratory environment for their adaptation before experiments. Food was supplied according to their daily schedule and water *ad libitum*. Carrageenan was (100 µl of 3% w/v) injected by a

30 gauge needle into the upper palpebral region of the rabbit eye after instilling Proparacaine HCl Ophthalmic Solution USP (0.5%) for local anesthesia [36, 37]. Acute inflammation induced by carrageenan is believed to be disappeared within 24 h [38, 39]. A small piece of film formulation (VHD) was sterilized by UV exposure for 10 min at a distance of 25 cm from UV source and placed in the cul-de-sac carefully after 1 h of the injection when redness in the eye was noticed [18]. The anti-inflammatory activity was examined by the reduction of redness and tear discharge.

3 Results and discussion

All the films were found of uniform thickness in between 85 and 125 μm and are appropriate for ocular application [40]. Folding endurance value of >200 suggested enough strength and durability of the films [30]. Moisture content of the films varied from 5.52 to 7.67% at laboratory ambient condition. Where, the presence of PEG 400 (VHP) contributed to a higher moisture content than the

Table 1: Physicochemical properties of ocular film.

Film code	Plasticizer (20% w/w)	Moisture content (%)	RH (75%)	Thickness (μm)	Folding endurance
VHT	Triethanolamine	5.52 ± 0.47	11.22 ± 0.44	84.2 ± 0.005	>200
VHD	Dimethyl sulfoxide	6.85 ± 0.75	15.72 ± 0.54	110.8 ± 0.004	>200
VHP	Polyethylene glycol 400	7.67 ± 1.13	13.74 ± 0.49	125.2 ± 0.002	>200

others. The physical properties are given in Table 1. The moisture uptake of the film containing TEA (VHT) was slightly less (11.32% w/w at 75% RH) in comparison with that of the other films (VHD and VHP) at the same RH.

3.1 Swelling and erosion study

Swelling profile of the VID film as a function of time till 6 h has been depicted in Figure 1. Hydration and erosion after 6 h of swelling in presence of simulated tear fluid have also been exhibited in Figure 2. Hydration and erosion are the controlling factors of drug release particularly in gel-forming thin matrix film formulation. Values of swelling rate, K_s (174–363 h^{-1}), hydration level after 6 h of swelling (1684–2845%) and rate of erosion (16.16–24.12%) of the films are the dominating factors in the process of drug release. The film VHT has shown maximum swelling rate (K_s) of 363 h^{-1} compared to other formulation of VHD and

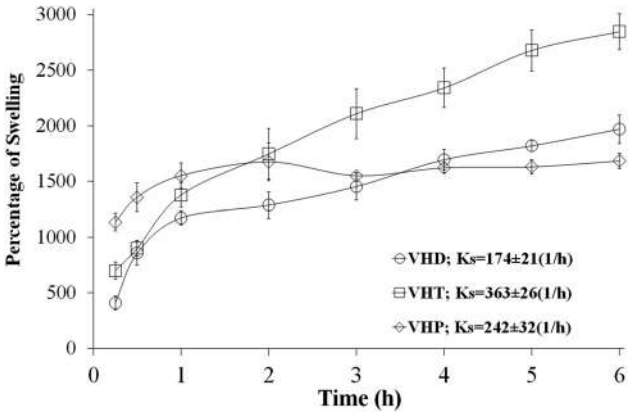

Figure 1: Swelling profile of VID film formulation containing DMSO TEA and PEG 400 as plasticizer.

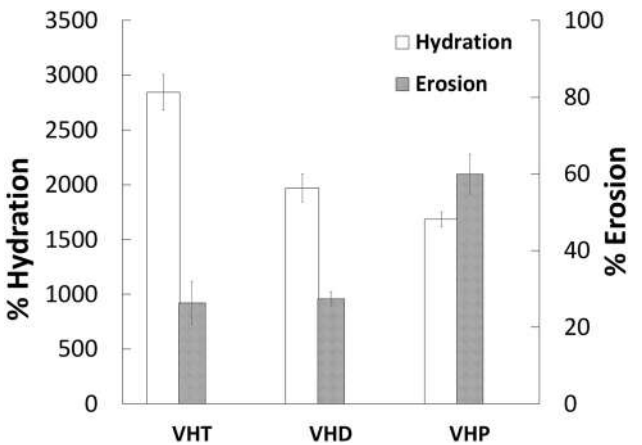

Figure 2: Hydration and erosion after 6 h of swelling in presence of simulated tear fluid.

VHP (174 and 242 h^{-1} respectively). The same film VHT exhibited least rate of erosion due to the presence of triethanolamine as the plasticizer rather than that of others containing DMSO and PEG 400. That means that swelling rate and hydration level are inversely related with the rate of erosion.

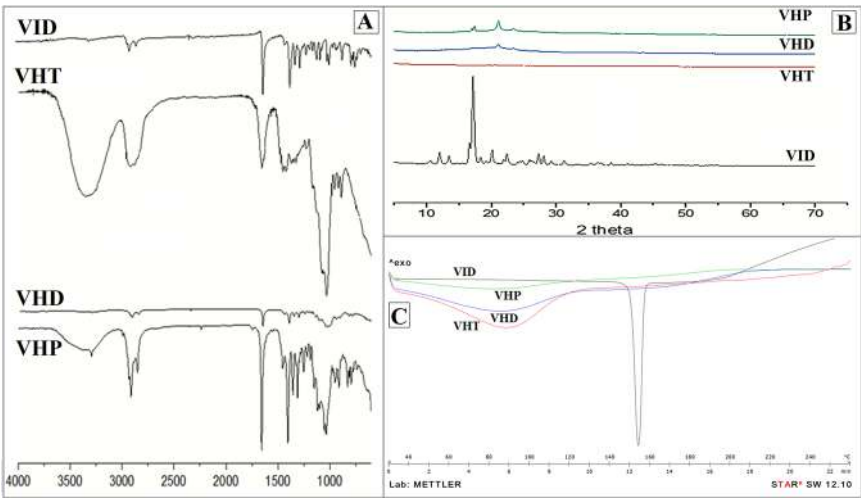

Figure 3: FTIR, DSC, and XRD study of VID and formulated films.

3.2 Fourier transform infrared spectroscopy

The characteristic peaks in the FTIR spectra of vildagliptin attributed to OH and N–H stretching vibrations were found at 3011–3370 and 3294 cm^{-1} respectively (Figure 3A). The peaks at 1663 and 1248 cm^{-1} were assigned to amide C=O, and C–N stretching [41, 42]. Vildagliptin containing film formulations showed a lower intensity peak of amide C=O stretching compared to the drug and a broad band in the region of 4000–3000 cm^{-1} probably because of OH stretching vibration of the intermolecular hydrogen bonds between polymer and drug. Incompatibility issue between the drug and the polymers may be ruled out as no significant change has been observed.

3.3 X-ray diffractometry

The XRD of VID and the formulations are represented in Figure 3B. The crystalline pattern showed characteristic peaks of the pure drug [43]. Vildagliptin showed intense characteristic peaks at 10.99, 12.45, 16.21, 19.15, 21.43, 26.33 and 28.30 2θ [41].

In the film formulations, VHT, VHD and VHP, the diffraction peaks were almost absent, representing the disappearance of crystals may be due to the presence of HPMC as the crystal growth inhibiting matrix polymer [44].

3.4 Differential scanning calorimetry

DSC of VID and all formulations are depicted in Figure 3C. A sharp endothermic peak of the pure vildagliptin was observed at 152.04 °C [45]. Due to moisture

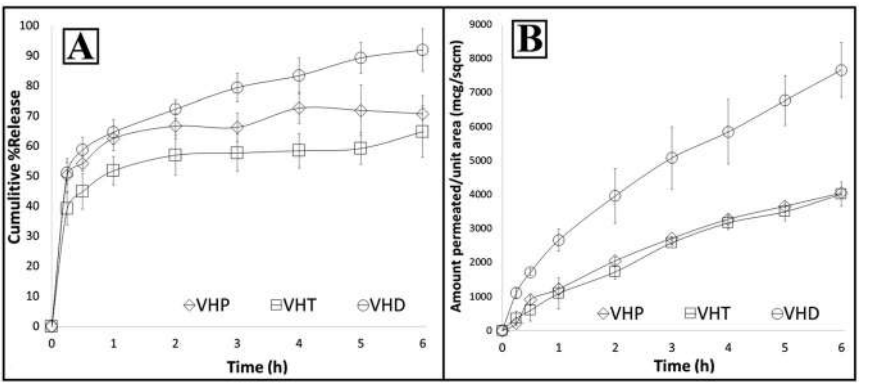

Figure 4: *In vitro* drug release and *ex vivo* permeation study of the film formulations.

evaporation from the polymeric matrix, a broad endothermic peak was found in the thermogram in the range of 60–110 °C [40, 46]. In the film formulations the sharp endothermic peak was absent, which established that the drug was almost completely amorphized.

3.5 *In vitro* drug release

In vitro release pattern has been presented in Figure 4A. The release initiated with a high rate may be due to the presence of HPMC as the hydrogel forming polymer matrix [47, 48]. Initially, the release of vildagliptin in the first hour was found to be more than 50% (51.8–65.5%) and reached to 64.8–91.9% at 6 h. DMSO plasticizer containing film (VHD) exhibited fastest release throughout compared to triethanolamine and polyethylene glycol 400 plasticized film formulations (VHT and VHP respectively).

Table 2: *In vitro* and *ex vivo* kinetics and permeation parameters.

Film code	*In vitro* release					Tissue permeation					Permeation parameters	
	First order	Higuchi		Peppas		First order	Higuchi		Peppas		J_s (μg/min)	$P_{ss} \times 10^2$ (cm/min)
	r^2	K	r^2	n	r^2	r^2	K	r^2	n	r^2	(mean ± sd) (n = 3)	(mean ± sd) (n = 3)
VHT	0.825	19.24	0.976	0.159	0.973	0.937	44.17	0.992	0.751	0.999	463 (94)	1.15 (0.001)
VHD	0.946	20.74	0.983	0.175	0.983	0.972	39.72	0.998	0.645	0.999	867 (54)	2.16 (0.002)
VHP	0.955	21.82	0.990	0.187	0.996	0.935	41.87	0.990	0.643	0.995	438 (38)	1.09 (0.001)

J_s = flux; P_{ss} = Permeability co-efficient.

3.6 *Ex vivo* permeation study

A sustained pattern of *ex vivo* permeation was observed from all the formulations (Figure 4B) because of the presence of lipophilic epithelial layer in the cornea. VHD showed maximum cumulative amount permeated throughout the period of 6 h than that of other formulations due to presence of DMSO as the plasticizer. DMSO might have interacted with the lipids of epithelial layer of cornea facilitating the permeation.

As per fitting of model test, it is understood that the kinetics of drug release and corneal permeation have followed both Higuchi and Korsmeyer-Peppas model (r^2 values in the range of 0.973–0.999) compared to relatively poor fitting with first order model (r^2 in the range of 0.825–0.972) as summarized in Table 2. The '*n*' values were found to be in the range of 0.159–0.187 (<0.5) depicting the probability of diffusion controlled release system [30]. In the case of *ex vivo* permeation study the obtained *n* values from the regression line of Korsmeyer-Peppas model were found in the range of 0.643–0.751 which is the evident of the system being partially

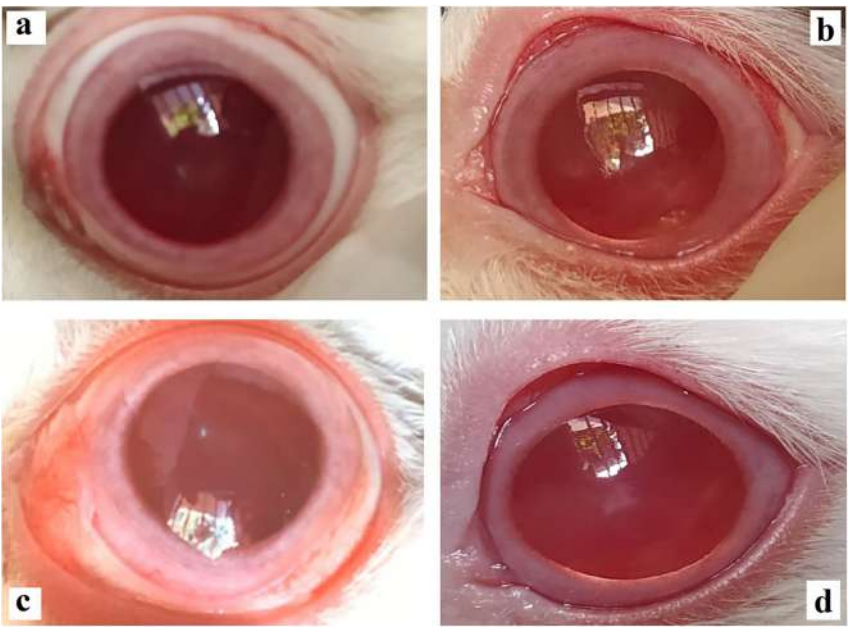

Figure 5: (a) Eye indicating no inflammation (b) after 45 min induce carrageenan eye appear redness and swelling (c) VID solution induced the rabbit eye in the cul-de-sac (d) untreated eye after 2 h.

diffusion and partially erosion controlled. Gel strength of the HPMC matrix film might have affected to some extent due to mucoadhesion during the corneal permeation and brought about partial erosion of the film [49]. Increased flux (J_s) and increased permeability co-efficient (P_{ss}) of VHD have also been resulted because of augmented permeation (867 μg/min and 2.16 cm/min respectively) compared to other films.

3.7 Anti-inflammation study

The normal and the inflamed eye are depicted in Figure 5a and 5b respectively. Significant lacrimation, reddening and swelling of the conjunctiva were noticed due to inflammation of the eye (Figure 5b). The redness of the rabbit eye almost disappeared within 2.5 h in the case of the treated one (Figure 5c). Whilst, symptoms of ocular inflammation continued to exist beyond 2.5 h in the untreated positive control rabbit eye (Figure 5d).

4 Conclusion

Triethanolamine, dimethyl sulphoxide, or polyethylene glycol 400 as plasticizer has been used successfully in HPMC based ocular film formulation of vildagliptin. Hydration level of swelling, swelling and erosion rate of the gel-forming thin matrix film played the controlling factor in the process of drug release, ocular residence and permeation. Maximum swelling rate of 363 h^{-1} has been exhibited by VHT compared to other formulation of VHD and VHP (174 and 242 h^{-1} respectively). The DSC and XRD study confirmed the absence of solid crystal structure of vildagliptin and presence of almost amorphized form in the film formulation. FTIR study has shown intermolecular hydrogen bonding between the polymer and the drug. The formulation containing DMSO (VHD) has shown highest *in vitro* release and *ex vivo* corneal permeation compared to other films. Ocular anti-inflammation of vildagliptin was observed by using VHD film formulation in the carrageenan induced ocular rabbit model. Plasticized vildagliptin film formulation could be utilized in the control and management of ocular inflammation in diabetic patients particularly with diabetic retinopathy after proper clinical studies with higher animal and human individual.

Acknowledgments: The authors are grateful to the Department of Science & Technology, Ministry of Science & Technology, New Delhi, India, for providing INSPIRE fellowship to Souvik Nandi (IF 180534). The authors are also very much

grateful to the President, Siksha O Anusandhan (Deemed to be University) for providing other facilities. The authors are also grateful to Glenmark Pharmaceutical Ltd. For the gift sample of vildagliptin.
Author contributions: All the authors have accepted responsibility for the entire content of this submitted manuscript and approved submission.
Research funding: None declared.
Conflict of interest statement: The authors declare no conflict of interest.

References

1. Shimodaira M., Niwa T., Nakajima K., Kobayashi M. Beneficial effects of vildagliptin on metabolic parameters in patients with type 2 diabetes. *Endocr. Metab. Immune Disord. – Drug Targets* 2015,*15*, 223–228.
2. Wang X., Hausding M., Weng S. Y., Kim Y. O., Steven S., Klein T., Daiber A., Schuppan D. Gliptins suppress inflammatory macrophage activation to mitigate inflammation, fibrosis, oxidative stress, and vascular dysfunction in models of nonalcoholic steatohepatitis and liver fibrosis. *Antioxidants Redox Signal.* 2018, *28*, 87–109.
3. Sudhakaran C., Kishore U., Anjana R. M., Unnikrishnan R., Mohan V. Effectiveness of sitagliptin in Asian Indian patients with type 2 diabetes—an Indian tertiary diabetes care center experience. *Diabetes Technol. Therapeut.* 2011, *13*, 27–32.
4. Kalra S. Emerging role of dipeptidyl peptidase-IV (DPP-4): inhibitor vildagliptin in the management of type 2 diabetes. *J. Assoc. Phys. India*. 2011, *59*, 237–245.
5. Yazbeck R., Howarth G. S., Abbott C. A. Dipeptidyl peptidase inhibitors, an emerging drug class for inflammatory disease. *Trends Pharmacol. Sci.* 2009, *30*, 600–607.
6. Wu Z., Wang S., Jin X., Bi Y., Ma S., Liu T. MiR-29a protects against cerebral ischemia injury by targeting DPP4 through TGF-β signaling pathway. *J. Neurosurg. Sci.* 2020, *64*, 586–587.
7. Chaudhuri A., Dandona P., Fonseca V. Cardiovascular benefits of exogenous insulin. *J. Clin. Endocrinol. Metab.* 2012, *97*, 3079–3091.
8. Forouhi N. G., Wareham N. J. Epidemiology of diabetes. *Medicine* 2010, *38*, 602–606.
9. Cho N., Shaw J. E., Karuranga S., Huang Y., da Rocha Fernandes J. D., Ohlrogge A. W., Malanda B. IDF Diabetes Atlas: global estimates of diabetes prevalence for 2017 and projections for 2045. *Diabetes Res. Clin. Pract.* 2018, *138*, 271–281.
10. Donath M. Y., Ehses J. A., Maedler K., Schumann D. M., Ellingsgaard H., Eppler E., Reinecke M. Mechanisms of β-cell death in type 2 diabetes. *Diabetes* 2005, *54*(Suppl. 2), S108–S113.
11. Ferreira L., Teixeira-de-Lemos E., Pinto F., Parada B., Mega C., Vala H., Pinto R., Garrido P., Sereno J., Fernandes R., Santos P. Effects of sitagliptin treatment on dysmetabolism, inflammation, and oxidative stress in an animal model of type 2 diabetes (ZDF rat). *Mediat. Inflamm.* 2010, *2010*; https://doi.org/10.1155/2010/592760.
12. Pollack R. M., Donath M. Y., LeRoith D., Leibowitz G. Anti-inflammatory agents in the treatment of diabetes and its vascular complications. *Diabetes Care* 2016, *39*(Suppl. 2), S244–S252.
13. Dobrian A. D., Ma Q., Lindsay J. W., Leone K. A., Ma K., Coben J., Galkina E. V., Nadler J. L. Dipeptidyl peptidase IV inhibitor sitagliptin reduces local inflammation in adipose tissue and in pancreatic islets of obese mice. *Am. J. Physiol. Endocrinol. Metab.* 2011, *300*, E410–E421.

14. Panina G. The DPP-4 inhibitor vildagliptin: robust glycaemic control in type 2 diabetes and beyond. *Diabetes Obes. Metabol.* 2007, (Suppl. 1), 32–39; https://doi.org/10.1111/j.1463-1326.2007.00763.x.
15. Katara R., Sachdeva S., Majumdar D. K. Aceclofenac oil drops: characterization and evaluation against ocular inflammation. *Pharmaceut. Dev. Technol.* 2017, *23*, 240–246.
16. Wirostko B., Mann B. K., Williams D. L., Prestwich G. D. Ophthalmic uses of a thiol-modified hyaluronan-based hydrogel. *Adv. Wound Care* 2014, *3*, 708–716.
17. Rocha E. D., Ferreira M. R. S., dos Santos Neto E., Barbosa E. J., Löbenberg R., Lourenço F. R., Bou-Chacra N. Enhanced in vitro antimicrobial activity of polymyxin B–coated nanostructured lipid carrier containing dexamethasone acetate. *J. Pharm. Innov.* 2020, *16*, 125–135.
18. Nanda A., Sahoo R. N., Pramanik A., Mohapatra R., Pradhan S. K., Thirumurugan A., Das D., Mallick S. Drug-in-mucoadhesive type film for ocular anti-inflammatory potential of amlodipine: effect of sulphobutyl-ether-beta-cyclodextrin on permeation and molecular docking characterization. *Colloids Surf. B Biointerfaces* 2018, *172*, 555–564.
19. Ariturk N. S., Oge I., Erkan D., Süllü Y., Şahin M. The effects of nasolacrimal canal blockage on topical medications for glaucoma. *Acta Ophthalmol. Scand.* 1996, *74*, 411–413.
20. Agrawal A. K., Das M., Jain S. In situ gel systems as 'smart'carriers for sustained ocular drug delivery. *Expet Opin. Drug Deliv.* 2012, *9*, 383–402.
21. El-Sousi S., Nácher A., Mura C., Catalán-Latorre A., Merino V., Merino-Sanjuán M., Díez-Sales O. Hydroxypropylmethylcellulose films for the ophthalmic delivery of diclofenac sodium. *J. Pharm. Pharmacol.* 2012, *65*, 193–200.
22. Mohapatra R., Senapati S., Sahoo C., Mallick S. Thermodynamic properties of ocular permeation of diclofenac: effect of triethanolamine. *FARMACIA* 2016, *64*, 72–81.
23. Bazuin C. G., Eisenberg A. Dynamic mechanical properties of plasticized polystyrene-based ionomers. I. Glassy to rubbery zones. *J. Polym. Sci, Part B: Polym. Phys.* 1986, *24*, 1137–1153.
24. Oh H. J., McGrath J. E., Paul D. R. Kinetics of poly(ethylene glycol) extraction into water from plasticized disulfonated poly(arylene ether sulfone) desalination membranes prepared by solvent-free melt processing. *J. Membr. Sci.* 2017, *524*, 257–264.
25. Panda B., Parihar A. S., Mallick S. Effect of plasticizer on drug crystallinity of hydroxypropyl methylcellulose matrix film. *Int. J. Biol. Macromol.* 2014, *67*, 295–302.
26. Hamid A., Khan M., Hussain F., Zada A., Li T., Alei D., Ali A. Synthesis and physiochemical performances of PVC-sodium polyacrylate and PVC-sodium polyacrylate-graphite composite polymer membrane. *Z. Phys. Chem.* 2021; https://doi.org/10.1515/zpch-2020-1763 [Ahead of Print/Just Accepted].
27. Swain K., Pattnaik S., Sahu S. C., Patnaik K. K., Mallick S. Drug in adhesive type transdermal matrix systems of ondansetron hydrochloride: optimization of permeation pattern using response surface methodology. *J. Drug Target.* 2010, *18*, 106–114.
28. Preis M., Woertz C., Kleinebudde P., Breitkreutz J. Oromucosal film preparations: classification and characterization methods. *Expet Opin. Drug Deliv.* 2013, *10*, 1303–1317.
29. Tanuma H., Saito T., Nishikawa K., Dong T., Yazawa K., Inoue Y. Preparation and characterization of PEG-cross-linked chitosan hydrogel films with controllable swelling and enzymatic degradation behavior. *Carbohydr. Polym.* 2010, *80*, 260–265.
30. Pramanik A., Sahoo R. N., Nanda A., Mohapatra R., Singh R., Mallick S. Ocular permeation and sustained anti-inflammatory activity of dexamethasone from kaolin nanodispersion hydrogel system. *Curr. Eye Res.* 2018, *43*, 828–838.

31. Kesarwani A., Yadav A. K., Singh S., Gautam H., Singh H. N., Sharma A., Yadav C. Theoretical aspects of transdermal drug delivery system. *Bull. Pharmaceut. Res.* 2013, *3*, 78–89.
32. Abdelrahman A. A., Salem H. F., Khallaf R. A., Ali A. M. Modeling, optimization, and in vitro corneal permeation of chitosan-lomefloxacin HCl nanosuspension intended for ophthalmic delivery. *J. Pharm. Innov.* 2015, *10*, 254–268.
33. Xu Y., Zhang C., Zhu X., Wang X., Wang H., Hu G., Fu Q., He Z. Chloramphenicol/sulfobutyl ether-β-cyclodextrin complexes in an ophthalmic delivery system: prolonged residence time and enhanced bioavailability in the conjunctival sac. *Expet Opin. Drug Deliv.* 2019, *16*, 657–666.
34. Abd-Elal R. M., Elosaily G. H., Gad S., Khafagy E. S., Mostafa Y. Full factorial design, optimization, in vitro and ex vivo studies of ocular timolol-loaded microsponges. *J. Pharm. Innov.* 2020, *15*, 651–663.
35. Fujishima H., Toda I., Yamada M., Sato N., Tsubota K. Corneal temperature in patients with dry eye evaluated by infrared radiation thermometry. *Br. J. Ophthalmol.* 1996, *80*, 29–32.
36. Mohapatra R., Mallick S., Nanda A., Sahoo R. N., Pramanik A., Bose A., Das D., Pattnaik L. Analysis of steady state and non-steady state corneal permeation of diclofenac. *RSC Adv.* 2016, *6*, 31976–31987.
37. Kato M., Hagiwara Y., Oda T., Imamura-Takai M., Aono H., Nakamura M. Beneficial pharmacological effects of selective glucocorticoid receptor agonist in external eye diseases. *J. Ocul. Pharmacol.* 2011, *27*, 353–360.
38. Fehrenbacher, J. C., Vasko, M. R., Duarte, D. B. Models of inflammation: carrageenan or complete freund's adjuvant (CFA) induced edema and hypersensitivity in the rat. *Curr. Protoc. Pharmacol.* 2012, *56*, 5.4.1–5.4.7.
39. Pattanaik S., Nandi S., Sahoo R. N., Nanda A., Swain R., Das S. Budesonide-cyclodextrin in hydrogel system: impact of quaternary surfactant on in vitro-in vivo assessment of mucosal drug delivery. *Rev. Chim. (Bucharest)* 2020, *71*, 332–345.
40. Mohapatra R., Senapati S., Sahoo C., Mallick S. Transcorneal permeation of diclofenac as a function of temperature from film formulation in presence of triethanolamine and benzalkonium chloride. *Colloids Surf. B Biointerfaces* 2014, *123*, 170–180.
41. Waghulde M., Naik J. Comparative study of encapsulated vildagliptin microparticles produced by spray drying and solvent evaporation technique. *Dry. Technol.* 2017, *35*, 1644–1654.
42. Nisar J., Iqbal M., Iqbal M., Shah A., Akhter M. S., Khan R. A., Uddin I., Shah L. A., Khan M. S. Decomposition kinetics of levofloxacin: drug-excipient interaction. *Z. Phys. Chem.* 2020, *234*, 117–128.
43. Kapor A., Nikolić V., Nikolić L., Stanković M., Cakić M., Stanojević L., Ilić D. Inclusion complexes of amlodipine besylate and cyclodextrins. *Cent. Eur. J. Chem.* 2010, *8*, 834–841.
44. Kumar Y. M., Bhagyasree K., Gopal N. O., Ramu C., Nagabhushana H. Structural, thermal and optical properties of Mn2+ doped methacrylic acid–ethyl acrylate (MAA: EA) copolymer films. *Z. Phys. Chem.* 2017, *231*, 1039–1055.
45. Baig M. M., Khan S., Naeem M. A., Khan G. J., Ansari M. T. Vildagliptin loaded triangular DNA nanospheres coated with eudragit for oral delivery and better glycemic control in type 2 diabetes mellitus. *Biomed. Pharmacother.* 2018, *97*, 1250–1258.
46. Castro-Hermida J. A., GóMez-Couso H., Ares-Mazás M. E., Gonzalez-Bedia M. M., CastañEda-Cancio N., Otero-Espinar F. J., Blanco-Mendez J. Anticryptosporidial activity of furan derivative G1 and its inclusion complex with beta-cyclodextrin. *J. Pharm. Sci.* 2004, *93*, 197–206.

47. Mura P., Zerrouk N., Faucci M. T., Maestrelli F., Chemtob C. Comparative study of ibuproxam complexation with amorphous β-cyclodextrin derivatives in solution and in the solid state. *Eur. J. Pharm. Biopharm.* 2002, *54*, 181–191.
48. Londhe V. Y., Umalkar K. B. Formulation development and evaluation of fast dissolving film of telmisartan. *Indian J. Pharmaceut. Sci.* 2012, *74*, 122–126.
49. Caccavo D., Cascone S., Lamberti G., Barba A. A., Larsson A. Swellable hydrogel-based systems for controlled drug delivery. *IntechOpen* 2016, *10*, 237–303.

Scientific paper

Influence of TiO_2 on Mucosal Permeation of Aceclofenac: Analysis of Crystal Strain and Dislocation Density

Souvik Nandi, Satyaki Aparajit Mishra, Rudra Narayan Sahoo, Rakesh Swain and Subrata Mallick*

School of Pharmaceutical Sciences, Siksha 'O' Anusandhan (Deemed to be University), Bhubaneswar, Odisha, India, 751003

** Corresponding author: E-mail: profsmallick@gmail.com; subratamallick@soa.ac.in*
Fax: +91-674-2350642, Tel: +91-674-2350635

Received: 05-22-2020

Abstract

Titanium dioxide can adhere with human epithelial cells and have good tolerability. Present work has been undertaken to explore the influence of TiO_2 on mucosal permeation of aceclofenac. Mucosal permeation of aeclofenac solution containing TiO_2 has been carried out. In fourier transform infrared spectrosopy (FTIR), the intensity of the peaks has decreased along with the increase of TiO_2 content in the formulation indicating a possible binding between drug and TiO_2. Melting enthalpy has been decreased with the increased content of TiO_2 in the solid. The status of crystal strain and dislocation density of TiO_2 and aceclofenac in the solid state formulation has also been evaluated from Xray Diffraction data using Debye-Scherrer's equation. Mucosal permeation of aceclofenac has shown sustained effect for more than 20 h in presence of titanium dioxide. Titanium dioxide could be used in designing formulation for sustaining mucosal aceclofenac delivery after performing risk assessment study.

Keywords: Aceclofenac; titanium dioxide; mucosal permeation; crystal strain; dislocation density; in vitro diffusion.

1. Introduction

Titanium Dioxide (TiO_2) is a biocompatible and stable material,[1] and has a wide range of application in various kinds of cosmetics. TiO_2 is accepted as food additive and also approved by Food and Drug Administration to be used in toothpaste, oral formulations etc.[2] Chen et al, 2011 described that TiO_2 is responsible for increasing intracellular Ca^{2+} concentration leading to elevated secretion of mucin.[3] TiO_2 coating is very much useful to adhere on epithelial tissues.[4] Masa and his colleagues, 2018 reported that TiO_2 has a property to attach with human epithelial cells along with a good tolerability.[5] TiO_2 nanoparticles interact instantly with the buccal mucosa upon contact and show a long residence time in the oral cavity.[6]

Aceclofenac is a widely used Biopharmaceutics Classification System (BCS) class II non-steroidal anti-inflammatory drug (NSAID).[7–9] It suffers from shorter elimination half-life and low oral bioavailability because of low aqueous solubility.[10–12] The toxic effects of this NSAID include gastric abnormalities like abdominal pain, gastric bleeding, dyspepsia etc. It is known that if the first pass metabolism is bypassed avoiding oral administration, improved bioavailability could be observed.[13] Aceclofenac eye drop has shown a marked reduction in ocular inflammation in post-operative cases of cataract operation.[14] Topical administration has been done frequently (2 hourly) for improved permeation through ocular mucosa. In vitro prolonged release has been studied for transmucosal delivery of aceclofenac using mucoadhesive dillenia fruit gum.[15] Katara et al., prepared a nano particle formulation of aceclofenac and claimed that the drug efficacy in local action can be improved if residence time of the formulation is amplified.[16]

In this present study the influence of TiO_2 has been explored on the mucosal permeation of aceclofenac in liquid formulation after topical administration. Any sort of sustained permeation of drug due to long residence time of TiO_2 upon interacting with the mucosal tissue has been examined. Solid state crystal strain and dislocation density have also been analysed.

2. Experimental

2. 1. Materials

Aceclofenac was received from Mannequin Pharmaceuticals Pvt. Ltd., (Bhubaneswar, India) as a gift sample. Titanium Dioxide was procured from Merck Specialities Pvt. Ltd, (Mumbai India).

2. 2. Preparation of Aceclofenac TiO_2 Kneaded Mixture

Aceclofenac was dissolved in a minimal amount of acetone and a kneaded mixture was prepared with titanium dioxide at different ratios (Table 1). [17,18] The mass was dried at 50 °C until constant weight and preserved in a desiccator.

2. 3. FTIR Study

KBR pellet method was used to carry out the FTIR study of pure drug and formulated powders.[19] A mean of 80 times was taken to obtain the average FTIR spectrum from 400 to 4000 cm^{-1} (Model: JASCO FTIR 4100 type A).

2. 4. DSC Study

Differential scanning calorimetry (DSC) cell was calibrated with Indium (melting point: 156.5 C, ΔH_{fus} = 28.54 J/g).[20] The thermogram was recorded under nitrogen atmosphere (50 ml/min) while taking a sample weighing between 4–6 mg in an aluminium crucible. The rate of heating was 10 °C/min and the upper limit was set as 200 °C. [21,22]

2. 5. XRD Study

X-ray diffraction pattern of pure aceclofenac and kneaded mixtures were subjected for XRD study. The scan was carried out at a speed of 1°/ min from 5–70° in Rigaku Ultima IV. CU was used as a source for Xray.

2. 6. *In vitro* Drug Release Study

In vitro drug diffusion study was done in both side open glass tube using dialysis membrane (HIMEDIA Dialysis Membrane-150) (surface area of diffusion = 1.54 cm^2). Acurately weighed amount of the powder samples were taken inside the diffusion tube with 2 ml of fresh liquid medium. The dialysis tube was placed in vessel containing 200 ml phosphate buffer (pH 7.4 at 34 ± 0.5 °C) under a paddle speed of 50 rpm.[23,24] Aliquot of 10 ml was drawn at particular time intervals and replaced with same volume of fresh medium. The absorbance was checked in a UV-Visible spectrophotometer (JASCO V-630 UV-Visible spectrophotometer) at 274 nm.

2. 7. *Ex vivo* Permeation Study

The similar diffusion system was used to study drug permeation through the corneal mucosa. Whole fresh eye ball of goat was brought from the local butcher shop. The cornea was carefully separated out along with 2 to 4 mm of surrounding sclera tissue and washed thoroughly. The cornea was tied tightly with thread along the circumference of vertical cylindrical diffusion tube to prevent any kind of leakage. Powder samples were taken inside the tube with 2 ml of fresh liquid medium and the tube was placed in vessel containing 200 ml phosphate buffer (pH 7.4 at 34 ± 0.5 °C) under a paddle speed of 50 rpm. The tubes were attached with paddle using adhesive tapes and paddles were put down as the as the cornea just touches the dissolution medium. Samples (10 ml) were withdrawn at 0.5, 1, 2, 3, 4, 5, 6, 7, 11, 20 h and replenished with 10 ml of fresh medium. The samples were filtered through 0.45 µm syringe driven filter and analysed by UV-Visible spectrophotometer. The studies of all formulations were performed in triplicate.[25]

3. Results and Discussion

3. 1. FTIR

As depicted in Figure 1, an intense peak was observed at 3317 cm^{-1} may be due to the amine group.[26] Peaks at 1715 and 1771 cm^{-1} may be formed due to stretch-

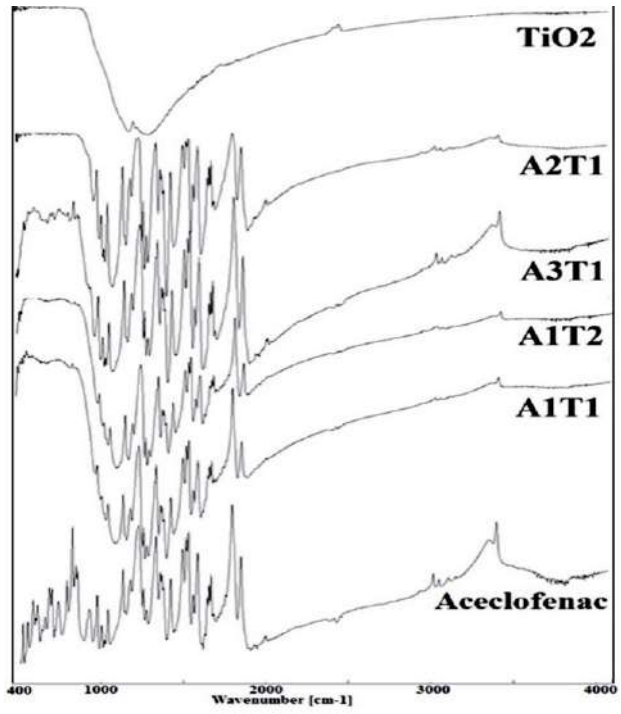

Figure 1. FTIR spectra of pure aceclofenac, TiO_2 and solid formulations.

ing of two carbonyl (C=O) groups in the drug structure.[27,28] The peak at 2969 cm^{-1} may be because of symmetric stretching of CH2 in both pure drug and formulations.[29] In the formulations, the intensity of the peaks has decreased along with the increase of TiO_2 indicating a possible binding between drug and TiO_2. The decrease of the peak intensity at 3317 with the increase of TiO_2 may be considered as the possible binding site with the oxygen present in titanium dioxide with the amine group of aceclofenac.

3. 2. DSC

The pure drug has shown a sharp melting point at 152.97 °C (Figure 2). The formulations have showed a ± 2 °C shifting of melting point along with lower peak intensity comparing to the pure drug. The pure drug has the highest enthalpy of melting (–155.76 jg^{-1}), where the enthalpy has reduced along with the decreased content of aceclofenac and increased content of TiO2 (Table 1). Probably the bond formation between TiO2 and aceclofenac is the cause of the decreased enthalpy of the formulations.

Table 1. Thermal behaviour of TiO_2 kneaded aceclofenac formulation

Formulation Code (Drug:TiO2)	Onset of Melting (°C)	Endset of Melting (°C)	Melting Point (°C)	Enthalpy (jg^{-1})
Aceclofenac	152.01	156.77	152.97	–155.76
A1T1 (1:1)	149.50	156.44	153.73	–62.11
A1T2 (1:2)	147.15	155.02	151.57	–32.23
A2T1 (2:1)	149.07	157.31	153.83	–66.67
A3T1 (3:1)	150.81	155.83	153.16	–153.09

3. 3. XRD Study

X ray diffraction data is portrayed in Figure 3. The TiO_2 as well as the formulations has shown a particular kind of diffraction pattern at 38.5° and 55° 2θ. The diffraction position and pattern proved that the TiO_2 anatase crystals has not changed in the formulations.[30] The most intense peaks then subjected to further calculation and an average value was taken as a representation for the whole formulation. The particle size was determined from the Debye-Scherrer's equation.[31]

$$D = \frac{K\lambda}{\beta Cos\theta} \quad (1)$$

Where, D is the crystal size (nm), K is a constant with a value of 0.9, λ is the wavelength of the Xray (0.1541 nm) and β is the value of FWHM (full width at half maxima) in radian. The X-ray diffraction pattern of TiO2 is evident to be at anatase phase[30,31] and the typical anatase TiO2 crystals have the octahedral structure.[32] Typically the K value can be considered as 0.9 and Anku et al., (2016) also estimated particle size of TiO2 anatase using Scherrer's Formula considering the shape factor 'K' as 0.9.[33]

Other characteristic properties of the formulations like, strain and dislocation density are tabulated in Table 2. Dislocation density can be described as the length of dislocation lines per unit volume of the crystals where dislocation is a linear defect found in crystals[34]. The untreated and treated pure TiO_2 has shown dislocation density of 0.80 and 0.71 respectively whereas the formulation with highest content of aceclofenac has shown almost 1.4 times higher dislocation lines per unit area. The similarity has also followed in the case of pure TiO_2 crystal strain (0.73) and the formulation, A3T1 has

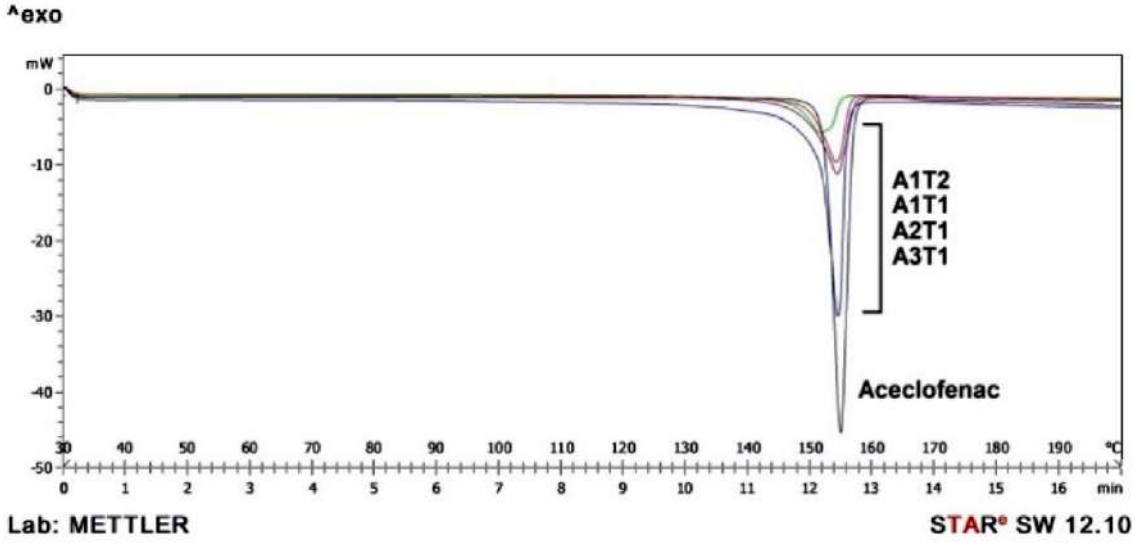

Figure 2. DSC Thermogram of aceclofenac and the formulations.

Table 2. Solid state particle properties of aceclofenac-titanium dioxide kneaded products

Formulation Code	TiO_2			Aceclofenac		
	Particle Size (nm)	Strain	Dislocation Density*10^{-3}	Particle Size (nm)	Strain	Dislocation Density *10^{-3}
Aceclofenac	–	–	–	98.08 ± 16.5	0.114 ± 0.014	0.44 ± 0.10
T1 (untreated TiO_2)	70.89 ± 3.64	0.073 ± 0.016	0.80 ± 0.088	–	–	–
T2 (Acetone treated TiO_2)	74.87 ± 1.60	0.068 ± 0.012	0.71 ± 0.030	–	–	–
A1T1	68.65 ± 0.84	0.075 ± 0.013	0.84 ± 0.021	73.47 ± 19.46	0.157 ± 0.037	0.90 ± 0.50
A1T2	64.44 ± 1.34	0.079 ± 0.015	0.96 ± 0.040	59.67 ± 11.56	0.132 ± 0.054	1.22 ± 0.40
A2T1	65.88 ± 3.15	0.077 ± 0.010	0.92 ± 0.092	71.09 ± 14.81	0.158 ± 0.054	0.98 ± 0.40
A3T1	63.01 ± 1.25	0.081 ± 0.013	1.00 ± 0.041	70.88 ± 14.58	0.149 ± 0.036	0.87 ± 0.30

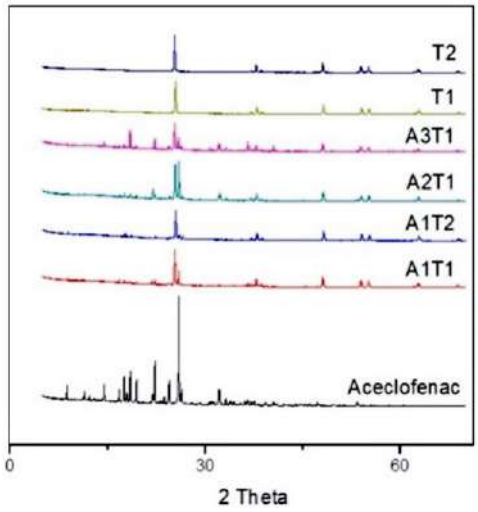

Figure 3. Powder Xray diffraction overlay of pure drug, formulation, untreated and treated titanium dioxide (T1 and T2 respectively).

shown the highest strain. The above mentioned changes may have occurred due to the binding of aceclofenac with titanium dioxide.[19] A similar phenomenon was noticeable in the case of aceclofenac where the dislocation density of A1T2 was higher than any other formulations or the pure drug itself. Particle size was found to be lowest in the case of the A1T2 formulation than the pure drug (98.08 nm).

3. 4. *In vitro* Diffusion Study

The observation was replicated in triplicate and the mean value is used to prepare the time vs cumulative percent release in Figure 4. The highest release was found in the case of A2T1 (89.88%) at 2 hours followed by A1T1 (89.13%). The formulation containing highest amount of TiO2 (A1T2) has shown lowest amount of drug release 82.55% in contrast to others at 120 mins.

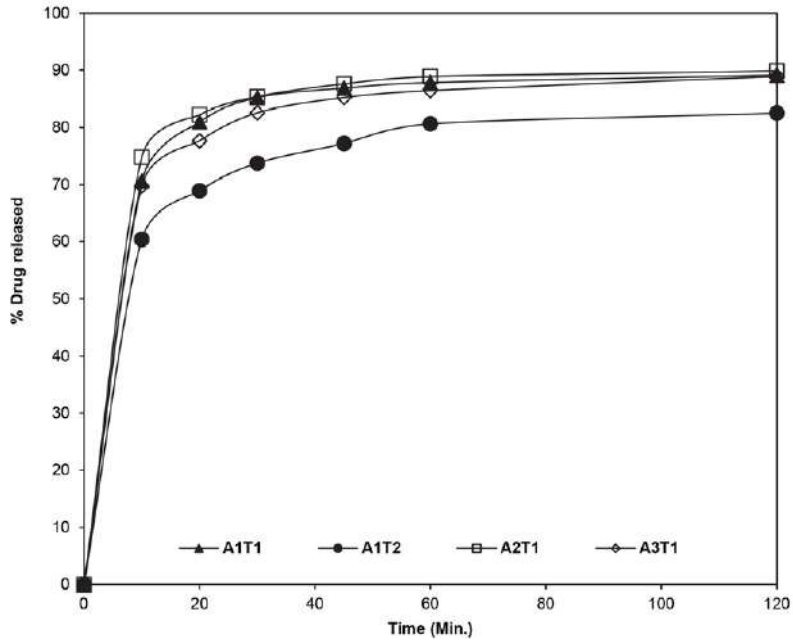

Figure 4. *In vitro* drug diffusion profile of the formulation

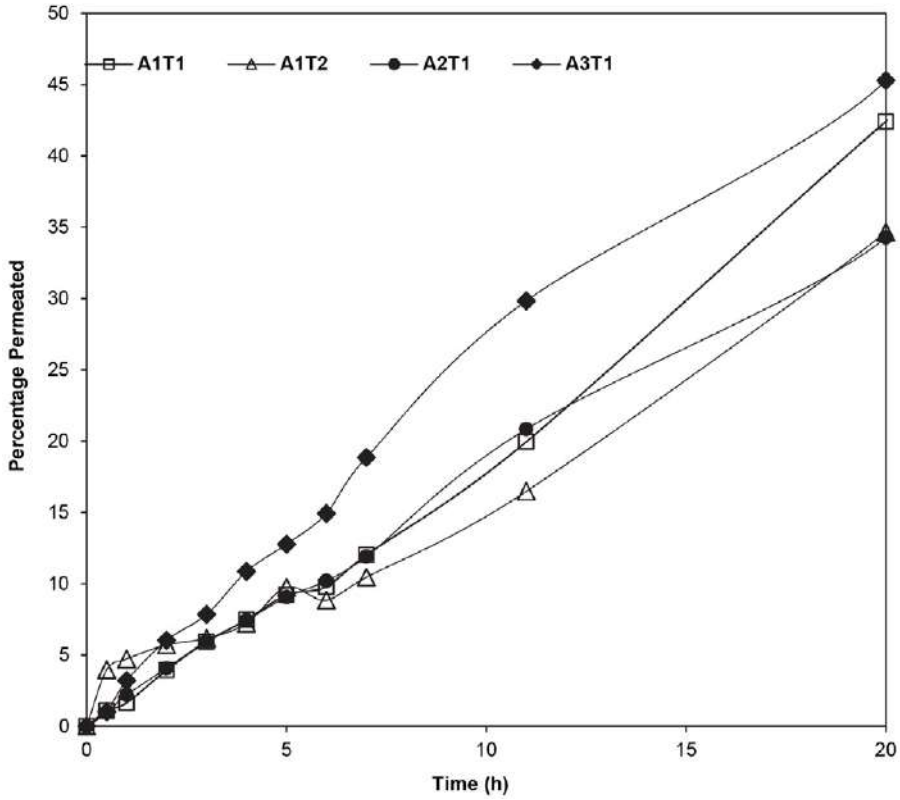

Figure 5. *Ex vivo* permeation study of the formulations through goat corneal mucosa

3. 5. *Ex vivo* Permeation Study

The data was presented as a plot of time vs percentage permeated in Figure 5. The highest release was found in the case of A3T1 (45.29 %) at 20 hours followed by A1T1 (42.40 %). In all of the formulations the permeation was continued up to 20 hours while maintaining an increasing order. Aceclofenac 0.1 % solution exhibited goat corneal permeation of almost 50–90 % within 2 h only in the pH range of 7–7.4.[14]

4. Conclusion

Influence of titanium dioxide on mucosal permeation of aceclofenac has been carried out in aqueous state. FTIR results revealed the decreased intensity of some characteristic peaks of aceclofenac in the formulation with the decreased content of aceclofenac and increased content of TiO_2 indicating possible binding between drug and TiO_2. Thermal analysis has also exhibited decreased melting enthalpy with the decrease of aceclofenac and increase of TiO_2 content in the solid. The change in crystal strain and dislocation density of TiO_2 and aceclofenac in the solid formulation has been noticed. Sustained mucosal permeation of aceclofenac has been observed for more than 20 h in presence of titanium dioxide. Titanium dioxide could be used in designing formulation for sustaining and controlling mucosal delivery of aceclofenac after assessing risk factor associated with TiO_2.

Acknowledgement

The authors are grateful to the Department of Science & Technology, Ministry of Science & Technology, New Delhi, India, for providing INSPIRE fellowship to Souvik Nandi (IF 180534). The authors are also grateful to Dr. Monojranjan Nayak, President, Siksha 'O' Anusandhan (Deemed to be University) for other laboratory facilities. We are also grateful to receive Aceclofenac as a gift sample from Mannequin Pharmaceuticals Pvt. Ltd., Bhubaneswar, Odisha. The authors are also grateful to the anonymous reviewers for their critical comments and suggestions to improve the quality of the manuscript.

Conflict of Interest

The authors declare no conflict of interests.

5. References

1. H. M. A. Shawish, H. Tamous, S. Saadeh, A. Tbaza, *Acta Chim. Slov*. **2018**, *65*, 811–822. **DOI:**10.17344/acsi.2018.4383
2. M. Skocaj, M. Filipic, J. Petkovic, S. Novak, *Radiol. Oncol.* **2011**, *45*, 227–247. **DOI:**10.2478/v10019-011-0037-0

3. E. Y. Chen, M. Garnica, Y. C. Wang, C. S. Chen, W. C. Chin, *PloS one*. **2011**, *6*, e16198. **DOI:**10.1371/journal.pone.0016198
4. S. Riivari, K. Shahramian, I. Kangasniemi, J. Willberg, T. O. Närhi, *Int. J. Oral Maxillofac. Implants*. **2019**, *34*, 313–319. **DOI:**10.11607/jomi.6862
5. R. Masa, Á. Deák, G. Braunitzer, Z. Tóth, J. Kopniczky, I. Pelsőczi-Kovács, K. Ungvári, I. Dékány, K. Turzó, *J. Nanosci. Nanotechnol*. **2018**, *18*, 3916–3924. **DOI:**10.1166/jnn.2018.15261
6. B. J. Teubl, G. Leitinger, M. Schneider, C. M. Lehr, E. Fröhlich, A. Zimmer, E. Roblegg, *Nanotoxicology*, **2015**, *9*, 253–261. **DOI:**10.3109/17435390.2014.921343
7. T. Soni, C. Nagda, T. Gandhi, N. P.Chotai, *Dissolut. Technol.* **2008**, *15*, 31–35. **DOI:**10.14227/DT150208P31
8. M. Grau, J. Guasch, J. L. Montero, A. Felipe, E. Carrasco, S. Juliá, *Arzneim-Forsch Drug Res*, **1991**, *41*, 1265–1276.
9. N. Sethuraman, S. Shanmuganathan, K. Sandhya, B. Anbarasan, *Indian J. Pharm. Educ.* **2018**, *52*, 581–586. **DOI:**10.5530/ijper.52.4.67
10. R. Raj, P. Mongia, A. Ram, N. K. Jain, *Artif Cells Nanomed. Biotechnol*. **2016**, *44*, 1434–1439.
11. https://pubchem.ncbi.nlm.nih.gov/compound/Aceclofenac#section=Melting-Point
12. B. Tubić, A. Uzunović, S. Pilipović, Ž. Gagić, *Acta Chim. Slov*. **2016**, *63*, 193–9. **DOI:**10.17344/acsi.2015.2168
13. S. Korani, M. Korani, S. Bahrami, T. P. Johnston, A. E. Butler, M. Banach, A. Sahebkar, *Drug Discov. Today*. **2019**, *24*, 567–574. **DOI:**10.1016/j.drudis.2018.09.023
14. V. Dave, S. Paliwal, *Saudi Pharm. J*. **2014**, *22*, 240–245. **DOI:**10.1016/j.jsps.2013.03.001
15. M. S. Hasnain, P. Rishishwar, S. Ali, A. K. Nayak, *SN App. Sci.* **2020**, *2*, 1–8. **DOI:**10.1007/s42452-019-1756-x
16. R. Katara, D. K. Majumdar, *Colloid Surface B*. **2013**, *103*, 455–462. **DOI:**10.1016/j.colsurfb.2012.10.056
17. A. Modi, P. Tayade, *AAPS PharmSciTech*. **2006**, *7*, E87. **DOI:**10.1208/pt070368
18. S. Nandi, S. A. Mishra, R. N. Sahoo, R. Swain, S. Mallick, *Indian J. Pharm. Educ.* **2020**, *54*, 68–72. **DOI:**10.5530/ijper.54.1.8
19. M. Starsinic, R. L. Taylor, P. L. Walker Jr, P. C.Painter, *Carbon*. **1982**, *21*, 69–74. **DOI:**10.1016/0008-6223(83)90158-6
20. G. Vanden, V. B. F.Mathot, *Thermochim. Acta*. **2006**, *446*, 41–54. **DOI:**10.1016/j.tca.2006.02.022
21. R. N. Sahoo, A. Nanda, A. Pramanik, S. Nandi, R. Swain, S. K. Pradhan, S. Mallick, *Acta Chim. Slov.* **2019**, *66*, 923–933. **DOI:**10.17344/acsi.2019.5139
22. M. Acharya, S. Mishra, R. N. Sahoo, S. Mallick, *Acta Chim. Slov.* **2017**, *64*, 45–54. **DOI:**10.17344/acsi.2016.2772
23. S. A. Agnihotri, T. M. Aminabhavi, *J. Control. Release.* **2004**, *96*, 245–259. **DOI:**10.1016/j.jconrel.2004.01.025
24. M. S. Bhandari, S. M. Wairkar, U. S. Patil, N. R. Jadhav, *Acta Chim. Slov*, **2018**, *65*, 492–501. **DOI:**10.17344/acsi.2017.3822
25. M. S. Kaynak, M. Celebier, S. Sahin, S. Altinöz, *Rev. Chim. (Bucharest).* **2013**, *64*, 27–30.
26. R. Mohapatra, S. Senapati, C. Sahoo, S. Mallick, *Farmacia*. **2016**, *64*, 72–81.
27. C. Y. Won, C. C. Chu, J. D. Lee, *Polymer*, **1998**, *39*, 6677–6681. **DOI:**10.1016/S0032-3861(98)00032-9
28. W. J. Ray, J. E. Katon, B. Phillips, *J. Mol. Struct.* **1981**, *74*, 75–84. **DOI:**10.1016/0022-2860(81)80009-9
29. P. S. Thomas, J. Guerbois, G. F. Russell, B. J.Briscoe, *J. Therm. Anal. Cal.* **2001**, *64*, 501–508. **DOI:**10.1023/A:1011578514047
30. A. Di Paola, M. Bellardita, B. Megna, F. Parrino, L. Palmisano, *Catal. Today.* **2015**, *252*, 195–200. **DOI:**10.1016/j.cattod.2014.09.012
31. W. Anku, S. O. Oppong, S. K. Shukla, P. P. Govender, *Acta Chim. Slov.* **2016**, *63*, 380–391. **DOI:**10.17344/acsi.2016.2385
32. S. Yang, N. Huang, Y. M. Jin, H. Q. Zhang, Y. H. Su, H. G. Yang, *Cryst. Eng. Comm.*, **2015**;*17*, 6617–6631. **DOI:**10.1039/C5CE00804B
33. A. Bishnoi, S. Kumar, N. Joshi, in: Microscopy Methods in Nanomaterials Characterization, Elsevier, **2017**, pp. 313–337. **DOI:**10.1016/B978-0-323-46141-2.00009-
34. I. Boukhoubza, M. Khenfouch, M. Achehboune, B. M. Mothudi, I. Zorkani, A. Jorio, in: *J. Phy.: Conference Series*, IOP Publishing, **2019**, *1292*, 012011. **DOI:**10.1088/1742-6596/1292/1/012011

Povzetek

Titanov dioksid se lahko adherira na človeške epitelijske celice in se dobro prenaša. Opisano delo je proučevalo vpliv TiO_2 na prepustnost sluznice za aceklofenak. Izvedena je bila študija prepustnosti sluznice za raztopino aceklofenaka, ki je vsebovala TiO_2. Pri infrardeči spektroskopiji s Fourierjevo transformacijo (FTIR) se je intenzivnost vrhov zmanjšala hkrati s povečanjem vsebnosti TiO_2 v formulaciji, kar kaže na morebitno vezavo med učinkovino in TiO_2. Entalpija taljenja se je zmanjšala s povečanjem vsebnosti TiO_2 v trdni snovi. Stanje kristalne oblike in dislokacijska gostota TiO_2 in aceklofenaka v trdni formulaciji sta bila ocenjena iz podatkov rentgenske difrakcije z uporabo Debye-Scherrerjeve enačbe. Prepustnost sluznice za aceklofenak je v prisotnosti titanovega dioksida pokazala podaljšano delovanje za več kot 20 ur. Titanov dioksid bi se po izvedbi študije ocene tveganja lahko uporabil pri oblikovanju formulacije za zadrževanje acekolofenaka na sluznici.